Received: 17 February 2023 | Revised: 7 August 2023 | Accepted: 17 August 2023

DOI: 10.1002/esp.5698

RESEARCH ARTICLE

ESPL WILEY

Nearshore ice complex breakup is controlled by a balance between thermal and mechanical processes

Ethan J. Theuerkauf[1] | Lucas K. Zoet[2,3] | Stefanie E. Dodge[2] | William Tuttle[2] | J. Elmo Rawling III[4]

[1]Department of Geography, Environment, and Spatial Sciences, Michigan State University, East Lansing, Michigan, USA

[2]Department of Geoscience, University of Wisconsin-Madison, Madison, Wisconsin, USA

[3]Department of Civil and Environmental Engineering, Geological Engineering Program, University of Wisconsin-Madison, Madison, Wisconsin, USA

[4]Wisconsin Geological and Natural History Survey, University of Wisconsin-Madison, Madison, Wisconsin, USA

Correspondence
Ethan J. Theuerkauf, Department of Geography, Environment, and Spatial Sciences, Michigan State University, East Lansing, MI, USA.
Email: theuerk5@msu.edu

Funding information
National Science Foundation, Grant/Award Numbers: 1916179, 1950101

Abstract

Shore ice is an important facet of cold-climate coastal geomorphology yet is generally understudied in comparison to other aspects such as nearshore hydrodynamics. Climate change is resulting in more dynamic shore ice regimes (i.e., shortened ice season and multiple freeze–thaw cycles); thus, a clear understanding of the role of shore ice in coastal geomorphic evolution is needed. The presence of shore ice is generally thought to provide the coast a protective buffer from storm waves though some studies have indicated enhanced nearshore erosion and sediment transport associated with ice development. This is particularly apparent during the breakup phase of shore ice as sediment can be scoured from the bed, deposited in place, or transported offshore. Given this, understanding the mechanics of shore ice breakup is critical. This study documents the first combined field and laboratory evaluation of the physical conditions leading to shore ice breakup, detailing the complex interplay between thermal and mechanical processes in ice deterioration. Through a wave tank experiment as well as field observations, wave impacts alone are shown to be unlikely to cause breakup of shore ice and thermal weakening is required. This has important implications both for predicting when ice will break up as well as for identifying potential nearshore sediment transport pathways. If ice breaks up entirely from thermal degradation, then sediment is likely to be deposited in place, whereas if ice breaks up from a combination of thermal degradation and wave impact, then sediment can be redistributed across the shoreface. Monitoring of meteorological conditions during ice breakup can likely be used as a first-order predictor of geomorphic changes resulting from shore ice deterioration.

KEYWORDS
coastal geomorphology, coastal sediment transport, shore ice, wave tank

1 | INTRODUCTION

Cold coasts cover 30% of the world's coastlines and often have large Indigenous populations (Lantuit et al., 2011); however, they have received minimal research attention in coastal geomorphology. Ice along the shoreline (i.e., shore ice) is characteristic of these cold coast regions and can be present as fast-ice attached the shoreline, drift ice floating in the nearshore or large bodies of ice ridges and lagoons that extend outward from the shoreline known as the nearshore ice complex (NIC). As the global climate warms, cold coasts will be disproportionately affected by rising atmospheric and water temperatures through the reduced spatial and temporal extent of shore ice (Irrgang et al., 2022). Areas that were once permanently frozen or seasonally frozen will transition to a shortened shore ice season or multiple ice growth and decay events. This alteration in the relative magnitude and timing of shore ice processes will have ramifications for nearshore sediment budgets and long-term geomorphic evolution of cold-climate coasts (Farquharson et al., 2018; Nielsen et al., 2022;

Theuerkauf et al., 2021) because nearshore sediment transport mechanisms (i.e., alongshore and cross-shore transport) are modified by the presence of ice (e.g., Barnes et al., 1993, 1994; Forbes & Taylor, 1994). Overall, the formation of nearshore ice significantly impacts the dynamics of nearshore sediment transport in cold regions (BaMasoud & Byrne, 2012). When shore ice is present, typical beach and nearshore processes are essentially shut down or shifted offshore until ice breakup. During breakup, substantial amounts of sediment can be moved with the ice, and the nature of this transport is largely dictated by the physical conditions occurring during breakup, which are not well constrained (Barnes et al., 1994; Dodge et al., 2022; Miner & Powell, 1991). Through a combined field and laboratory approach, this study addresses the fundamental question of what factors lead to shore ice breakup and what that means for potential sediment transport and geomorphic change.

1.1 | NIC characteristics and impacts on nearshore processes

The NIC forms along wave-dominated cold coastlines and is characterized by an icefoot attached to the beach and a sequence of ice ridges and ice lagoons extending basinward (Figure 1; Marsh et al., 1973; Evenson & Cohn, 1979; Barnes et al., 1994). Nearshore ice freezes to the beach, initially forming an icefoot that causes waves to break either atop or basinward of the frozen zone, which minimizes erosion and transport of beach sediment (Evenson & Cohn, 1979; Marsh et al., 1973; Miner & Powell, 1991). After this stable platform of frozen material is built in the shallow zone the NIC can extend offshore as a series of ridges separated by flat ice lagoons. As wave action increases, floating brash and slush ice is thrust up onto either the ice lagoon or the icefoot depending on the antecedent conditions. This overwash of ice and associated sediment builds the characteristic ice ridges of the NIC, which are often, though not always, associated with nearshore bars due to wave breaking (Bajorunas & Duane, 1967; Seibel et al., 1976). As the ice front grows into deeper water it can inhibit below-ice wave action and associated sediment transport, nearly eliminating it in the cross-shore direction while reducing the flow velocities (and thus shear stresses) in the alongshore direction to rates too low to entrain and transport bedload particles (Manson et al., 2016). The NIC builds from the shoreline basinward during the winter months and in some instances may form and breakup multiple times throughout the ice season.

The formation of the NIC has two major impacts on the nearshore morphology and sediment budget: (1) It can protect the beach and dunes from erosive storm waves (e.g., BaMasoud & Byrne, 2012; Marsh et al., 1973), and (2) the ice that makes up the NIC can entrain sediment and upon breakup raft debris out into deeper waters, possibly beyond the depth of closure (e.g., Barnes et al., 1994; Miner & Powell, 1991). These geomorphic impacts can vary considerably from year to year depending on the spatial and temporal variability in shore ice cover. In some years, when ice is extensive and present for the entire winter, minimal shoreline and beach areal change are documented (BaMasoud & Byrne, 2012; Evenson & Cohn, 1979; Mattheus et al., 2019). However, in other years massive net sediment movement can occur if no or minimal shore ice is present (e.g., Theuerkauf et al., 2021). Although previous research has defined these end members of change, little is known about the mechanics of sediment transport during breakup events and how that relates to whether the net impact of shore ice presence is erosive or protective.

1.2 | Present understanding of NIC breakup

NIC destruction typically occurs in late winter and early spring; however, in the more southern latitudes of cold-climate coasts

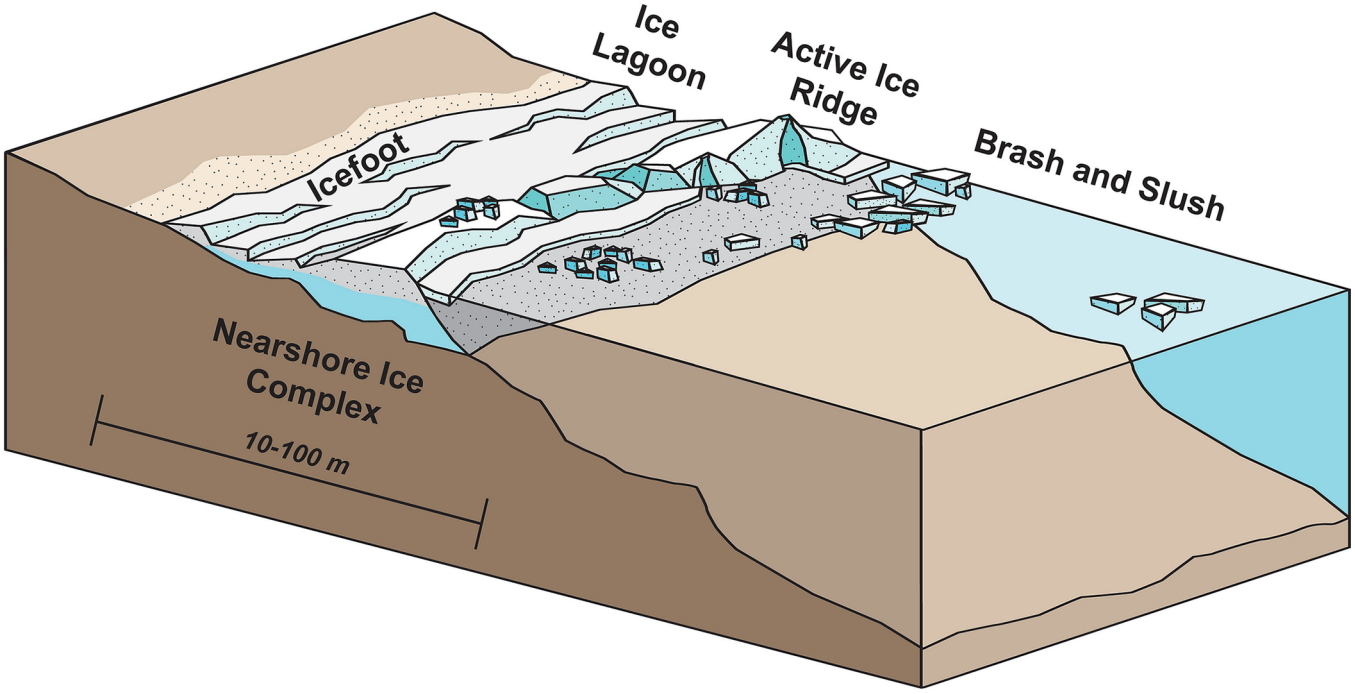

FIGURE 1 Conceptual diagram of the components of the nearshore ice complex (NIC).

(e.g., southern portions of the Great Lakes of North America) NIC breakup may occur multiple times throughout the winter. Previous studies indicate that NIC decay is a function of either thermal (e.g., ice melting) (Bryan & Marcus, 1972; Marsh et al., 1973) or mechanical breakup via waves (e.g., Miner & Powell, 1991; O'Hara & Ayers, 1972). Additionally, previous work on shore ice in the Arctic Sea indicates that weakening of ice due to enhanced solar radiation preconditions the ice to be broken apart by wave and current action (Petrich et al., 2012). The wide range of decay sequences and timings reported in these studies demonstrates the complexity of the ice breakup process. Marsh et al. (1973) show that ice lagoons melt first and then decay proceeds to the ridges, which are larger and likely grounded to the bars. They also allude to the importance of waves for breakup by reporting rapid ice decay associated with storm wave occurrence. Alternatively, O'Hara and Ayers (1972) document ice breakup beginning with the most offshore ridges and proceeding landward, primarily in response to wind wave action. Other studies, such as Miner and Powell (1991) and Barnes et al. (1994) support the notion that waves are the primary agent of NIC breakup and suggest that this is important for coastal sediment budgets.

The mechanism of NIC breakup has important implications on patterns and pathways of sediment transport. For example, if the NIC breaks up primarily by thermal processes, then the sediment entrained within the ice will likely be deposited in place, facilitating beach building (Marsh et al., 1973; O'Hara & Ayers, 1972). If thermal processes dominate, then large-scale NIC breakup can be predicted to occur during times of increasing atmospheric and/or water temperature largely independent of wave conditions. Although ocean or lake water has a greater ability to deliver heat to the NIC than the atmosphere, much of the NIC landward of the outermost ridge is hydraulically separated from the open waters; thus, an increase in atmospheric temperature can exchange large amounts of heat with the upper surface of the NIC producing abundant surface melt. This effect can be amplified if surface albedo is reduced due to sediment deposition within or on the ice, thus increasing the solar heat absorption (Bryan & Marcus, 1972). However, if the NIC breakup process is dominated by mechanical breakup from wave action, as it is predominantly reported in the literature, then the debris-laden ice has the potential to be transported out to deeper water where its sediment content can be deposited beyond the depth of closure (e.g., Barnes et al., 1994; Miner & Powell, 1991; O'Hara & Ayers, 1972). This implies that this sediment is removed from the nearshore system. Mechanical breakup can originate from the energy expenditure of wave action on the NIC exceeding the yield strength of the ice. This is most likely to occur when waves are large or when the ice is mechanically weak due to large numbers of preexisting fractures or thermal processes 'degrading' pieces of the ice. NIC breakup likely depends on some combination of the thermal and mechanical processes, but the fundamental question of which process is more important, how these processes work together and what this could mean for potential geomorphic processes remains.

The overarching question of what fundamentally controls NIC breakup is addressed by conducting a combined field and laboratory investigation. The study utilizes a time-series of drone-based aerial photographs and ground-based panoramic images along with wave and temperature data to evaluate the *in situ* conditions leading to NIC breakup. Then, experiments were conducted within a novel cryogenic wave tank for comparison with field observations and to ultimately determine the conditions most favorable for NIC breakup and the relative importance of thermal versus mechanical processes. The results are used to develop a conceptual model of the relationship between NIC breakup dynamics and the potential for nearshore sediment transport and coastal geomorphic change.

2 | METHODOLOGY AND METHODS

2.1 | Study area

The southern shore of Lake Superior is an ideal location to study the dynamics of NIC breakup because ice there typically forms in December, builds throughout the winter to a maximum in late February and early March and then breaks apart in April and May (Wang et al., 2018). The absence of multiple freeze–thaw events affords the opportunity to examine the mechanisms and geomorphic impacts of ice breakup without the confounding effects of variable ice extent throughout a winter season. In this region, the timing of ice breakup corresponds with the spring warming and storm season. This provides wave energy that mechanically erodes the ice while it warms and allows the effects of both thermal and mechanical processes to be examined.

Two sandy beach study sites along the southern Lake Superior coast were monitored to study the dynamics of ice breakup (Figure 2). Both sites have similar morphologies and are exposed to similar lake level and climatic conditions; however, they differ in terms of fetch and wave exposure. The furthest west site is located along the southwestern end of the Keweenaw Peninsula near Ontonagon, Michigan. This site is characterized by a ~20-m-wide sandy beach fronting a sandy bluff. Onshore waves approach from the west, with the northwest being the direction with the largest fetch. The eastern site is located within Marquette Bay in Chocolay Charter Township, just east of Marquette, Michigan. Similar to the Ontonagon site, the morphology is characterized by a 10- to 20-m-wide sand beach fronting a ~10-m-tall sandy bluff. Storm waves at the Chocolay site approach from northerly directions, with north being the direction of the largest fetch. At the time of the study, neither site had shore armoring that would alter coastal geomorphic processes.

To assess NIC breakup field-based ground and aerial observations were combined with laboratory-based experiments of NIC formation and breakup. NIC conditions were monitored at Ontonagon with repeat unoccupied aerial system (UAS) flights that were used to build orthomosaic images of NIC breakup. Ground-based photos were collected at the Chocolay site to document NIC breakup. For both locations, wave and temperature data were gathered from NOAA observations and models to compare to the observational data of NIC breakup. In addition to the field observations, experiments were conducted in a cryogenic wave tank to assess the relative importance and mechanics of thermal and mechanical processes for NIC breakup.

2.2 | Climate data

Significant wave height data were acquired for each study site using the nearest Great Lakes Coastal Forecasting System (GLCFS) model

FIGURE 2 (Left) Study area map depicting the location of the Chocolay and Ontonagon sites within the Great Lakes basin. (Right) Aerial photos of the two sites along the southern Lake Superior coast.

grid node. Archived Nowcast model data for the monitoring periods (25 February through 31 March 2021, for the Chocolay site and 17 February through 24 March 2021, for the Ontonagon site) were provided by the National Oceanic and Atmospheric Administration's Great Lakes Environmental Research Lab (NOAA-GLERL). All storm waves, which are defined in the Great Lakes as waves greater than 2 m (Hubertz, 1992), were identified to define potential periods of increased mechanical breakup of the NIC.

Atmospheric temperature data were accessed via Wunderground.com from weather stations near the two study sites for the same monitoring periods as the wave data. The Sawyer International Airport weather station is ~20 km southwest of the Chocolay site, and the Ontonagon County weather station is ~12 km southwest of the Ontonagon site. All periods of atmospheric temperatures above freezing (0°C) were identified and used to define potential periods of increased thermal breakup of ice.

2.3 | UAS flights

To study the breakup of the NIC at the Ontonagon site, a UAS was used to repeatedly image 11.16 ha during the winter of 2021 (Figure 2). A DJI Phantom Advanced 4 drone with a high-resolution 35 mm equivalent, f/2.8–f/11 camera collected high-resolution aerial imagery at the site on 17 February, 6 March, 10 March and 24 March. Map Pilot Pro was utilized to create a custom and repeatable flight path for each survey. Images were collected nadir with 67% overlap and 1.4-cm-per-pixel resolution. Individual images were geotagged using the UAS's onboard GPS with an accuracy of ~1 m.

The individual overlapping georeferenced images were combined and orthorectified to create a single georeferenced orthomosaic image for each survey (Westoby et al., 2012). For each flight, the CMOS (complementary metal oxide sensor) on the camera attached to the UAV auto adjusted the cameras aperture and shutter speed to match the appropriate lighting conditions. Once the flight was completed, the RAW images were exported to Map Pilot Pro's Maps Made Easy (MME) program for photo alignment. The MME software aligned and combined the images and generated orthomosaic imagery. These orthomosaics were exported as GeoTIFFs and imported into QGIS for a qualitative analysis of NIC breakup processes.

2.4 | Ground-based photos

Approximately daily offshore-facing panoramic images were collected from 25 February to 31 March 2021 at the Chocolay site. These images were collected using an Apple iPhone camera from a fixed location at the top of the bluff. Due to weather conditions or scheduling constraints, photographs were not collected every day; however, no more than two consecutive days are missing from the record. The individual images were stitched together using the Photomerge command in Adobe Photoshop CC and then exported as TIFFs for analysis.

2.5 | Wave tank

To individually assess the impacts of mechanical versus thermal processes on NIC breakup scaled models of the study beaches were created in a wave tank. A cryogenic wave tank (3 m long × 0.6 m wide × 1.2 m tall) was constructed in a large walk-in freezer to simulate cold coast processes (Figure 3). The air temperature of the freezer is controlled to within 0.5°C. A set of heating elements input heat at different locations of the water column to control water temperature

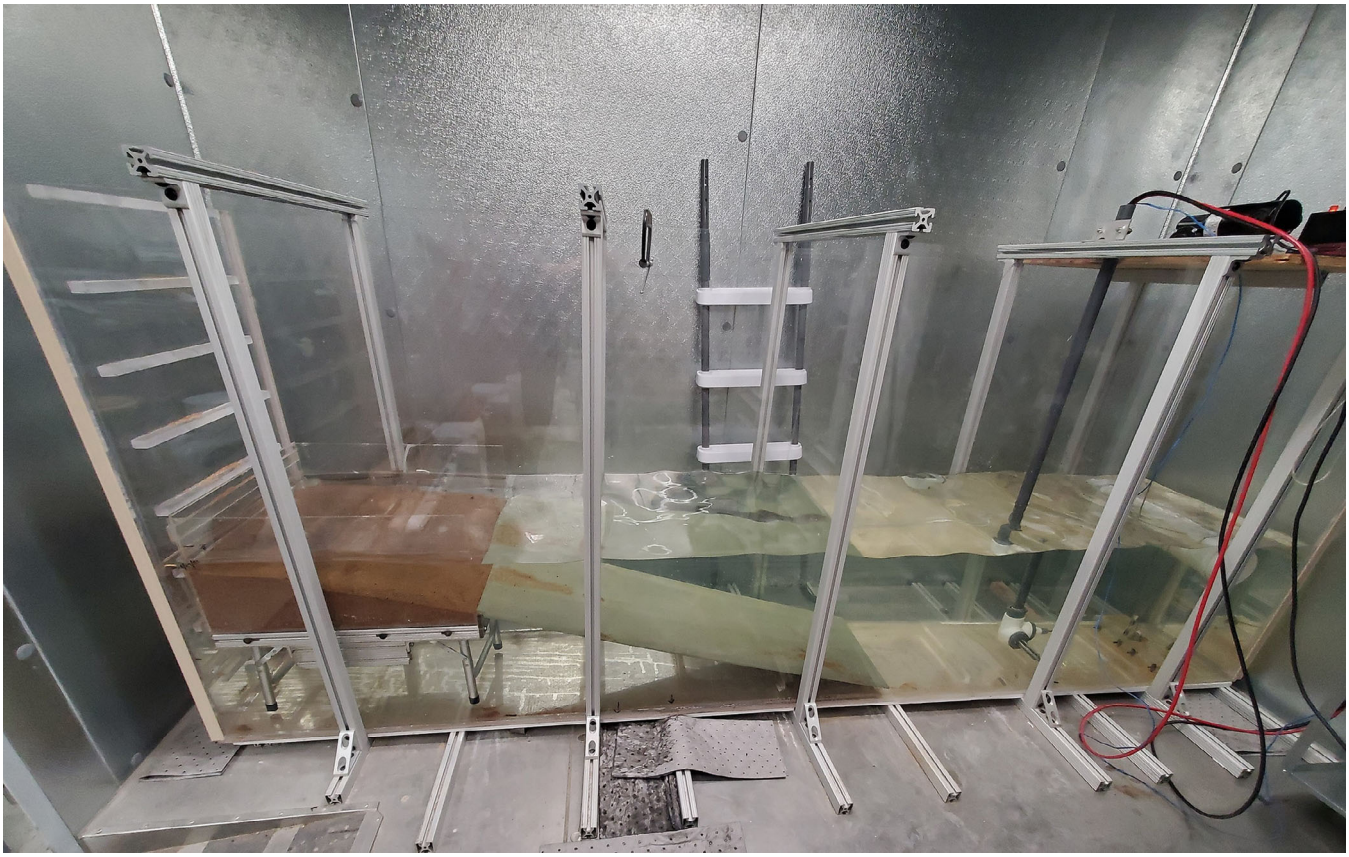

FIGURE 3 Side profile of the wave tank device. To the left of the photo is the beach ramp and the sediment beach. On the right side of the photo is the plunging wave generator and a heating element. When the tank is in use cameras are mounted to the overhead aluminum struts. The wave tank is located within a large walk-in freezer. The wave tank is 3 m long × 0.6 m wide × 1.2 m tall.

to within 0.1°C, which allows a wide range of air and water temperature combinations. The wave tank walls are constructed from 1.905 cm acrylic, which is structurally supported by an exoskeleton of aluminum struts. The water level in the tank is variable and at one end of the tank a plunging wave generator produces scaled surface waves with a range of adjustable wave periods and amplitudes. On the other end of the wave tank is a ramp with coarse-grained (0.788 mm mean diameter) sand that simulates the shoreface. Experimental conditions are continuously tracked with a variety of instruments. Wave period and amplitude are measured at several locations within the wave tank using a pressure transducer. In addition, two cameras track the passing waves in reference to a grid mounted on the tank wall. An overhead camera is used to take photos of the beach area at a regular interval for comparison with UAS field observations. A series of high precision glass bead thermistors (0.01°C accuracy) track temperature gradients within the water. Data output from all instruments are digitized and captured in LabVIEW for synchronization and export. The water level can be adjusted along with the wave period and amplitude to achieve Froude number similitude with deep-water waves.

An NIC was first built in the wave tank and then broken up thermally and/or mechanically. The first experiment was designed to isolate the effects of mechanical breakup of the NIC. The freezer temperature was set to −6°C, and the heating element in the bottom of the tank was set to 1°C. Waves with a wavelength and amplitude of ∼0.5 and 0.01 m were applied. The water depth within the wave tank was 0.43 m. Froude scaling for these waves correspond to a 23.3 m wavelength in the natural beach for water depths of 20 m. Once an active NIC had formed, larger waves were produced with a 55% increase in amplitude in an attempt to initiate the mechanical breakup process without raising the temperature. The second experiment focused on the combined thermal and mechanical breakup of the NIC. The freezer atmospheric temperature was set to −2°C, the wave generator produced waves with a wavelength and amplitude of 0.4 and 0.01 m, respectively. The water depth within the wave tank was 0.43 m. Froude scaling for these waves correspond to an 18.6 m wavelength in the natural beach for water depths of 20 m. Once the NIC had formed, the wave generator plunging speed was increased, roughly doubling the wave amplitude. This was meant to represent relatively wavy conditions during warming events. The freezer temperature was also raised gradually over a 24 h period to 3°C while holding the wave properties constant. Importantly, the focus of these experiments was to investigate the mechanisms of NIC breakup and not exactly match conditions observed in the field.

To relate mechanical breakup properties of the wave tank to those observed in the field a nondimensionalized value was estimated, $\Gamma = F_w/F_s$, which is the ratio of the force imparted from waves, F_w, to force required to fracture the NIC, F_s. The estimation of the force exerted by waves on the ice front follows analysis of Mitsuyasu (1962) where the force imparted on a wall by waves (F_w) can be estimated using the following expression:

$$F_w = C_w \rho g H_o W d, \quad (1)$$

where C_w is an experimentally determined wave force coefficient that depends on beach slope and wave steepness (here following Mitsuyasu, 1962, C_w was set to 4 for the wave tank and 2 for the field setting), ρ is the density of water (1000 kg m^{-3}), g is gravitational constant (9.81 m s^{-2}), H_o is the surface water wave height, W is the width of the ice wall and d is the depth of the water at the ice wall. The force required to break the ice in the NIC, F_s, is estimated by using the yield stress of ice, σ_y, (here = 1 MPa) multiplied by the cross-sectional area of the thinnest ice, h, which is often located in the ice lagoon.

$$F_s = \sigma_y W h \quad (2)$$

Values of Γ that approach unity should be likely to mechanically break. Thermal weakening will effectively lower h by reducing ice thickness but also reduce σ_y through degradation of the ice.

3 | RESULTS

3.1 | Atmospheric and hydrodynamic conditions

At the Ontonagon site, there was a general rise in air temperature throughout the monitoring period; however, surface water temperature did not begin to rise appreciably until the beginning of March 2021 (Figure 4). During late February, there were several periods when air temperature rose above freezing, yet the surface water temperature remained right at freezing. Around 10 March, the air temperature rose substantially (to ~16°C), which corresponded with an increase in surface water temperature just above freezing (~2°C). From 11 March through 19 March, both air temperature and surface water temperature remained around freezing. On 20 March, both air temperature and surface water temperature began to rise again. Air temperature rose to around 16°C and surface water temperature rose to around 4°C.

A similar pattern was observed at the Chocolay site with both air and water temperatures generally remaining at or below freezing from the beginning of the monitoring period to 7 March 2021 (Figure 4). The air temperature fluctuated more at the Chocolay site during this period than the Ontonagon site. Starting on 7 March, the air temperature rose to a maximum of 8°C above freezing for around a week and the water temperature began to rise above freezing as well. The air temperature stayed entirely above freezing until 12 March when it dropped to around −4°C for a day then rose to around 8°C on 13 March and then dropped again to around −4°C on 14 March. Given the brief nature of these air temperature fluctuations, surface water temperature remained generally unchanged. From 15 March through 19 March, air temperature was slightly above freezing and surface water temperature

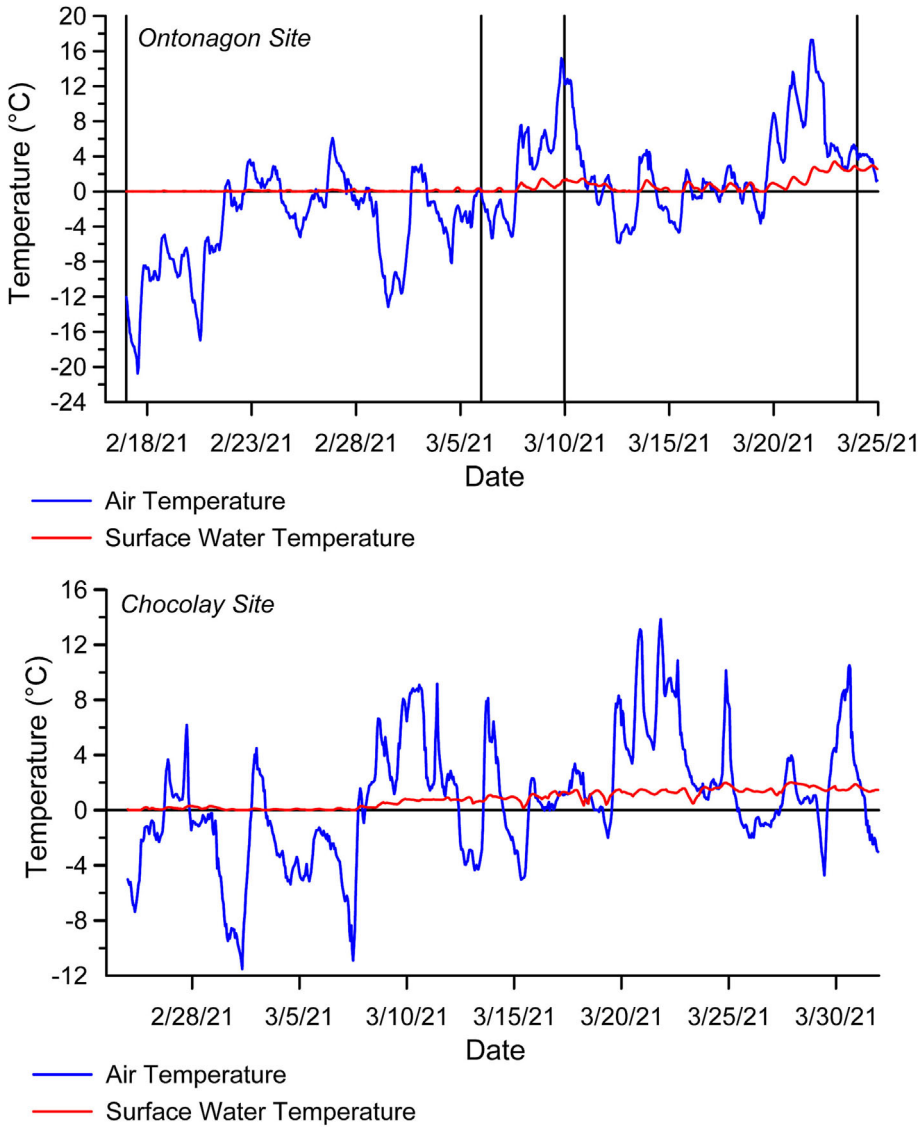

FIGURE 4 Air and water temperature records for both sites. Top panel contains the records for the Ontonagon sites with vertical black lines indicating the UAS survey times. Bottom panel contains the records for the Chocolay site.

remained steady. Air temperature rose rapidly on 20 March to a maximum just under 14°C and remained at this level until 23 March. Surface water temperature slowly rose throughout the rest of the monitoring period, whereas air temperature fluctuated periodically above and below freezing but generally remained above freezing.

Throughout the monitoring period, wave heights at both sites generally remained below the 2 m storm wave threshold. Wave heights during the first several weeks of monitoring at Ontonagon were less than a meter except for a brief period on 28 February and 1 March when waves rose to just over 1 m (Figure 5). The only period in the Ontonagon record when wave heights rose above 2 m was during an event on 11 and 12 March. From 12 March through the end of the monitoring period, wave heights remained below the storm threshold and generally below 1 m. The Chocolay wave height record was similarly devoid of any major storm events; however, periods of above 1 m waves appeared more frequently in the record than at the Ontonagon site. On 1 March and 12 March, wave heights briefly rose just above the storm wave height threshold. Otherwise, wave heights remained below this threshold with periodic increases to above 1 m, likely indicating low-magnitude onshore wind and wave events.

3.2 | UAS flights

The UAS flights provided snapshots of the NIC breakup process at the Ontonagon site that were linked to atmospheric and hydrodynamic conditions. The initial survey on 17 February 2021 documents a well-developed NIC with an outer ridge and an inner ridge separated by an ice lagoon (Figure 6). An inner ridge is present that coalesces with the grounded ice foot along parts of the site and appears to be separated from the icefoot by a small ice lagoon (Figure 6). A layer of featureless ice that is not considered part of the NIC is also present offshore of the outer ice ridge. On 6 March 2021, this flat ice offshore of the ridge had broken apart, presumably due to the low-magnitude wave event that occurred in early March, and only sheets and chunks of brash and slush where present in the imagery. Minimal change to the NIC was documented in this survey, though it appears that some melt could have occurred prior to the flight as accumulated sediment was exposed at the surface of the ridges. This accumulation of sediment could however also be the result of sublimation at the ice surface due to high sun intensity, even during sub-freezing air temperatures. By 10 March, substantial melting of the NIC was evident in the UAS imagery (Figure 6). Thinning of the ice in the lagoons was observed as well as melting along the ridges and icefoot, as evidenced by a super-accumulation of sediment along these features. During this time, no wave events were recorded, however, air temperature rose substantially (~10°C), and water surface temperature began to rise above freezing as well (~1–2°C). By 24 March 2021, most of the NIC had deteriorated through a combination of rising air and water surface temperatures as well as the wave event that occurred on March 11 and 12. The outer ice ridge was entirely removed, the lagoon separating the outer and inner ridge/icefoot thinned in some spots and

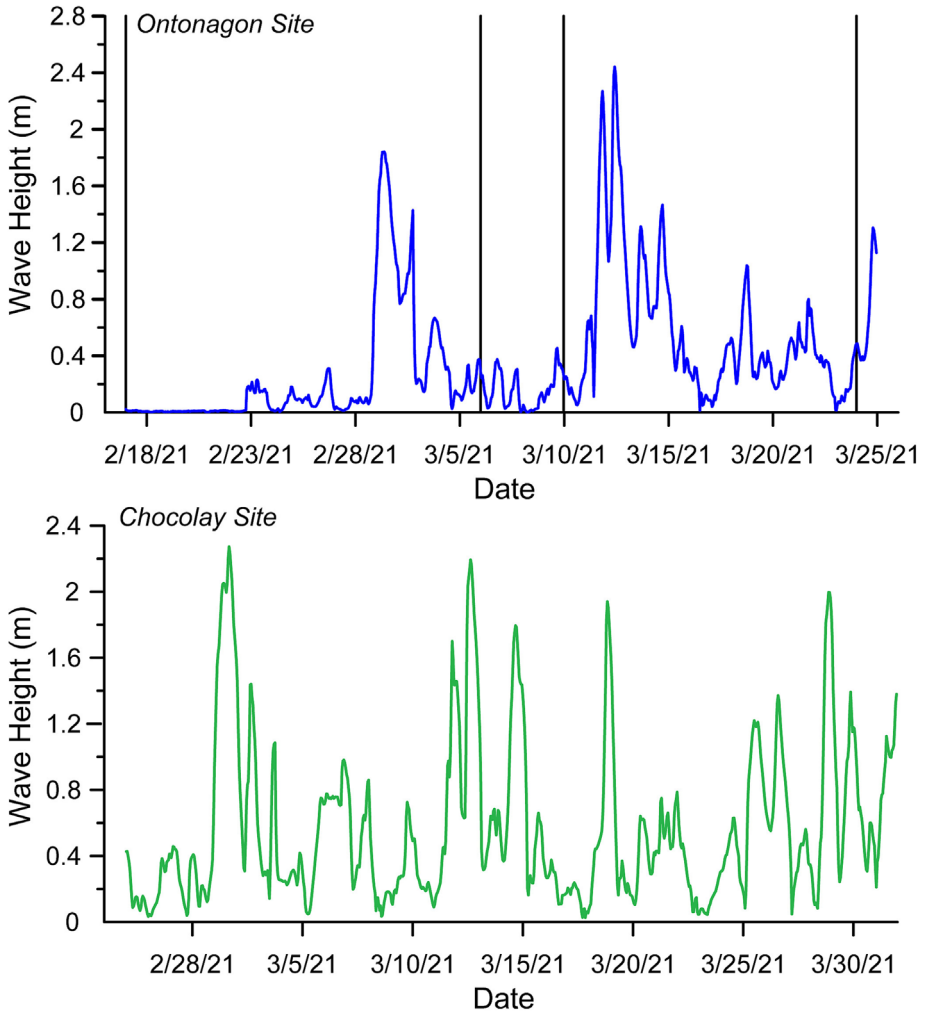

FIGURE 5 Significant wave height records for the Ontonagon (top) and Chocolay (bottom) sites. The dates of the UAS surveys at Ontonagon are depicted with black vertical lines.

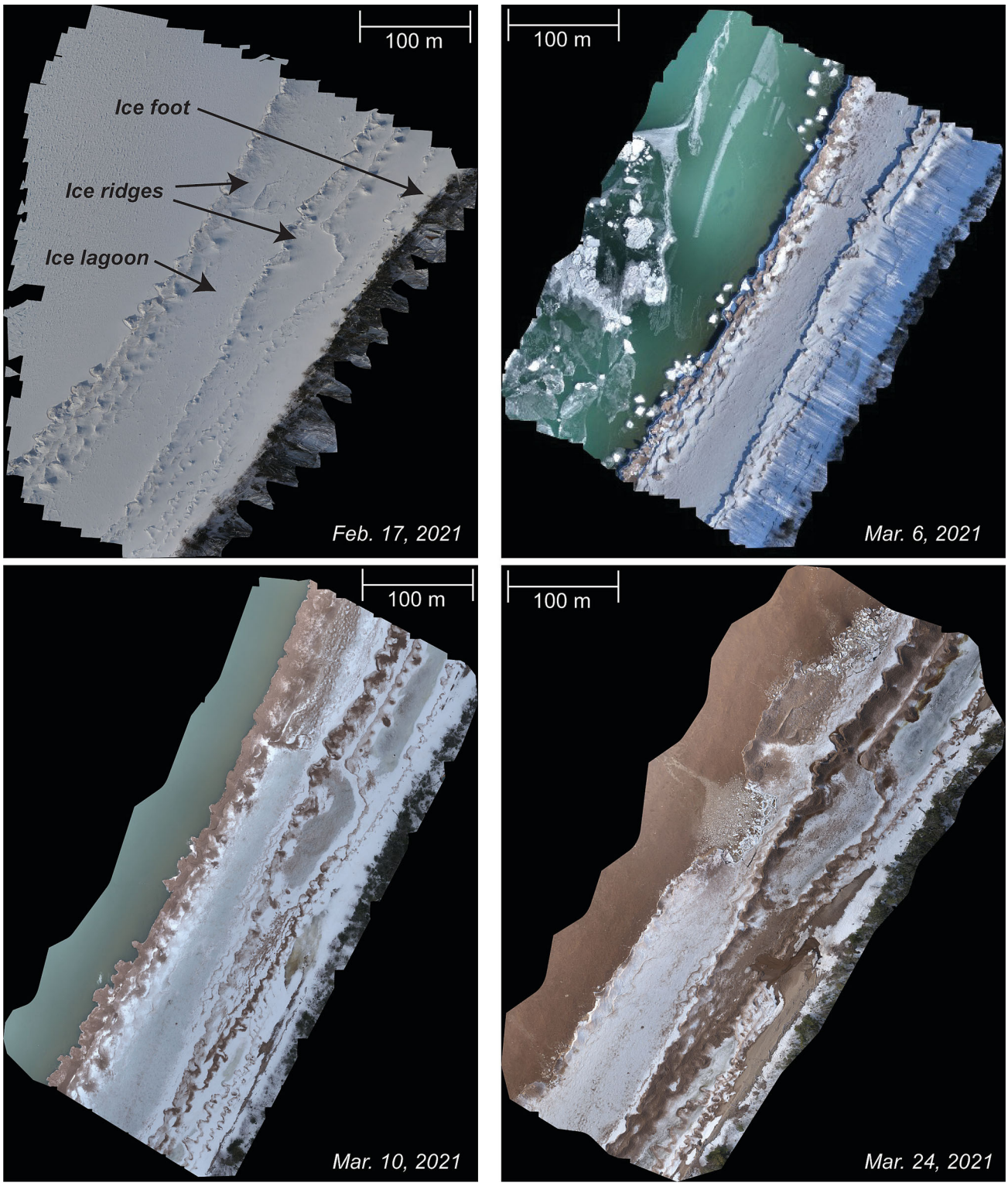

FIGURE 6 Orthomosaic images generated from the UAS flights at the Ontonagon site. (Top left) Full-developed NIC on 17 February 2021, (top right) 6 March 2021, (bottom left) 10 March 2021 and (bottom right) 24 March 2021.

broke apart in others, the inner ridge was thinning, and the icefoot had mostly decayed.

3.3 | Ground-based panoramic photographs

The panoramic imagery collected at the Chocolay site reveals similar ice breakup patterns as those documented in the UAS imagery at Ontonagon. The first image collected on 25 February 2021 depicts a moderately developed NIC with several sequences of ridges and intervening lagoons (Figure 7). The most landward lagoon is free of any ice and is located immediately offshore of the shoreline. On 1 March, a small storm event (peak wave height 2.3 m, Figure 5) impacted the site, but temperatures remained below freezing. This does not appear to have resulted in any breakup of the NIC but rather appears to have built up the outer ice ridge. The next day (2 March), the air

FIGURE 7 Panoramic images of initial NIC destruction at the Chocolay site from 25 February 2021 through 10 March 2021.

temperature rose to above freezing and while the waves were no longer characterized as storm waves, they remained above 1 m. Minimal change to the NIC occurred in response to these conditions. Air temperatures dropped to below freezing for the next several days and wave energy remained low (below 1 m). During this time, the NIC remained stable, and a thin layer of ice formed on the surface of Lake Superior far out into the basin.

Beginning on 7 March, the air temperature rose to above freezing and the ice lakeward of the NIC retreated (Figure 7). Temperatures remained above freezing until 12 March, and calm wave conditions (waves less than 1 m) were observed until 11 March. The photographs revealed that the NIC began to breakup on 9 March primarily from thermal effects given wave heights were less than 1 m (Figure 7). The in-place degradation of the NIC continued until 11 March when wave energy began to increase. Waves crossed the storm threshold on 12 March; however, the air temperature dropped to below freezing. The basinward portion of the NIC remained unchanged despite the increased wave energy and the ice lagoon closest to shore began to refreeze (Figure 7). Temperatures remained above freezing and wave heights were generally low from 13 March through 15 March, except for a 16 h period on 14/15 March where wave height was above 1 m yet below the storm threshold. The NIC deteriorated precipitously during this period, with just the shore-attached icefoot remaining on 15 March (Figure 7). Wave energy remained low, and temperatures were slightly above freezing during the period from 15 March and 18 March, and the extent of the NIC remained largely unchanged. On 18 March, wave height increased to just under the storm wave threshold and the last remaining portions of the NIC began to break apart (Figure 8). The following day air temperature rose above freezing until 25 March. The remaining NIC degraded in place during this period and by 22 March, only small bits of the NIC were left immediately adjacent to the shoreline (Figure 8). On 25 March, wave energy increased to above 1 m, and there was no evidence of any ice at the site. Although temperatures dropped to near freezing from 25 March through 28 March, no shore ice reformed.

3.4 | Wave tank

Experiment 1 formed a well-developed NIC with an inactive shore icefoot, an inactive ice lagoon, an active ice ridge and a mobile brush/slush zone (Figure 9; Supplementary Video S1). The morphologic

FIGURE 8 Panoramic images of final NIC destruction at the Chocolay site from 16 March 2021 through 25 March 2021. Sediment deposited in the shallow nearshore was visible in the 22 March 2021 image.

pattern of features observed in the experiment largely mimicked observations of the field photos. Time lapse imagery of the wave tank showed that the ice ridge was constructed from brash ice tossed atop the ice front during the ice building phase. The ice front grew to a water depth of 15 cm, and the minimal ice thickness located in the ice lagoon was ~1 cm. Experiment 2 also formed an active NIC, with an inactive shore icefoot, an active ice ridge and a mobile brush/slush zone (Figure 9; Supplementary Video S2). During buildup, however, a thin surface ice formed along the beach edge with water movement under the ice. This formation of a thin surface ice shelf differs from the ice formation in Experiment 1. Temperature and waves were altered from Experiment 1; hence, it is possible that the change in wavelength, wave height, the difference in the freezer temperature and the added base heat caused the different ice formations. The basinward extent of the ice was nearly the same as Experiment 1 as was the thickness of the ice in the lagoon.

The focus for Experiment 1 was to examine the ability of increased wavelength and amplitude to mechanically breakup the NIC without any change to the thermal conditions (i.e., the atmosphere temperature remained below freezing). Once a complete NIC was formed, the wave amplitude was approximately doubled to test if increased energy would lead to breakup. However, this change in wave amplitude resulted in further buildup offshore of the NIC. The purely mechanical attempt proved to be ineffective at initiating a NIC breakup under the conditions examined in the wave tank. With the largest waves produced the strength ratio, $\Gamma = 0.03$, indicating the waves were about 1/30 of the size needed to break apart the ice.

For Experiment 2, thermal and mechanical breakup conditions were created and the NIC was successfully broken apart (Figure 10). When the temperature was gradually raised to 3°C in the presence of moderate wave conditions, widespread thermal degradation of the NIC was induced leading to its complete destruction over ~20 h (Supplementary Video S2). During the destruction of the NIC the brash/slush ice zone first deteriorated leaving only the rigid shoreward components of the NIC intact (Figure 10). Following the melting of the brash ice, the grounded portion of the ridge began to deteriorate and became detached from the bed. Once the ridge was detached, water from the main basin was observed flowing under the ridge and ice lagoon in response to the wave action. This injection of warmer waters beneath the ice cap likely led to some component of sub-ice melt as warm water was flushed into the sub-ice cavity and cold water was drawn out. Once the outermost ice ridge had deteriorated the ice lagoon was relatively quickly destroyed. Prior to any wave action, the upper surface of the lagoon had several hours of

thermal degradation while the sub-ice section had undergone some thermal degradation from the cavity injection. The combination of these factors led the lagoon to deteriorate from both the basinward and shoreward side, ultimately breaking down and having the fragments flushed away by the modest wave action. Finally, after the ice ridge and the lagoon were both removed the ice foot broke up. This occurs from surface melt resulting from the greater than freezing atmospheric temperatures at first and then from the delivery of heat from the modest waves once all other components of the system had been removed. With the largest waves, the strength ratio in experiment two was $\Gamma = 0.03$, indicating the waves were again about 1/30 of the size needed to mechanically break apart the ice; however, this assumes that $h\sigma_y$ in the thermally weakened ice did not change from experiment one, which is certainly incorrect given that the ice did break apart. This implies that the ice had to have thinned and/or weakened in order to achieve the breakup that was documented during this experiment.

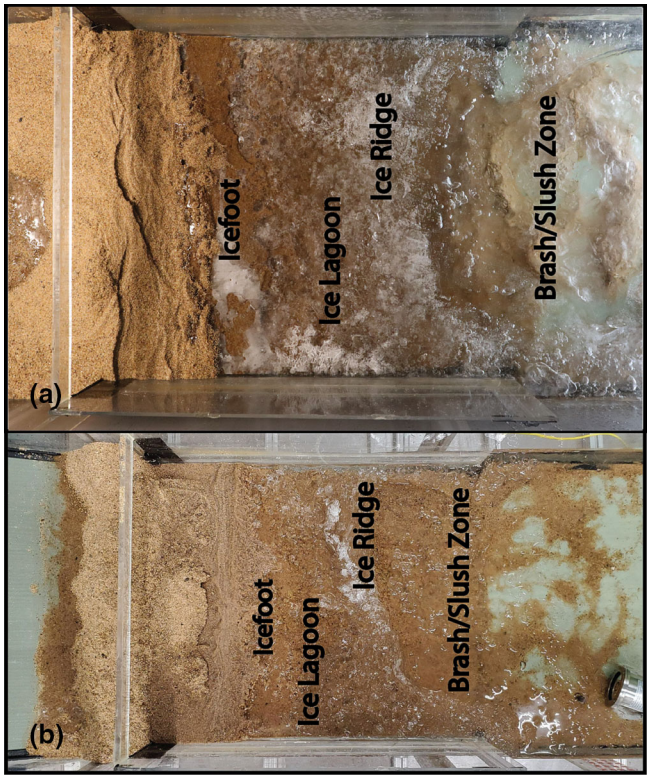

FIGURE 9 Overhead images of NIC development in the wave tank. Panel A is the developed NIC in Experiment 1, and Panel B is the developed NIC in Experiment 2. The width of the wave tank is 0.6 m in each image.

4 | DISCUSSION

4.1 | Processes of NIC breakup inferred from field data

At both field sites, the active ridge appears to first weaken from melting, which then allows destruction via wave action. Meteorologic and hydrodynamic data indicate that air and water temperatures rose at both sites during a period of low wave heights and active NIC deterioration. Two qualitative examples of ice weakening during rising temperatures were found in the Ontonagon imagery. First, oblique imagery collected along the active ice ridge indicates a lack of underlying ice to support the ridge (Supplementary Figure S1). Second, hinge deformation cracks formed along the ridges ranging from 2 to 20 cm (Supplementary Figure S2). These occur when mechanical torque acting on the NIC overcomes the strength of the ice and the cantilever portion breaks, similar to previous observations on dynamic river ice (Kelsch & Goldstein, 2010). Mechanical processes (i.e., wave action) facilitate the remaining breakup of the active ridge as it is exposed to open water. Once the active ridge is weak enough from melt and the mechanical forces from waves are sufficient, the destruction of the active ridge can occur rapidly (i.e., hours to days) as was observed at both sites in this study. Marsh et al. (1973) documented a similar situation where the entire NIC was destroyed in as little as 2 days. The sequence of processes leading to this breakup has important implications for dictating the net sediment transport impacts from ridge destruction. The advanced thermal weakening that occurred prior to wave attack appears to have caused sediment contained within the

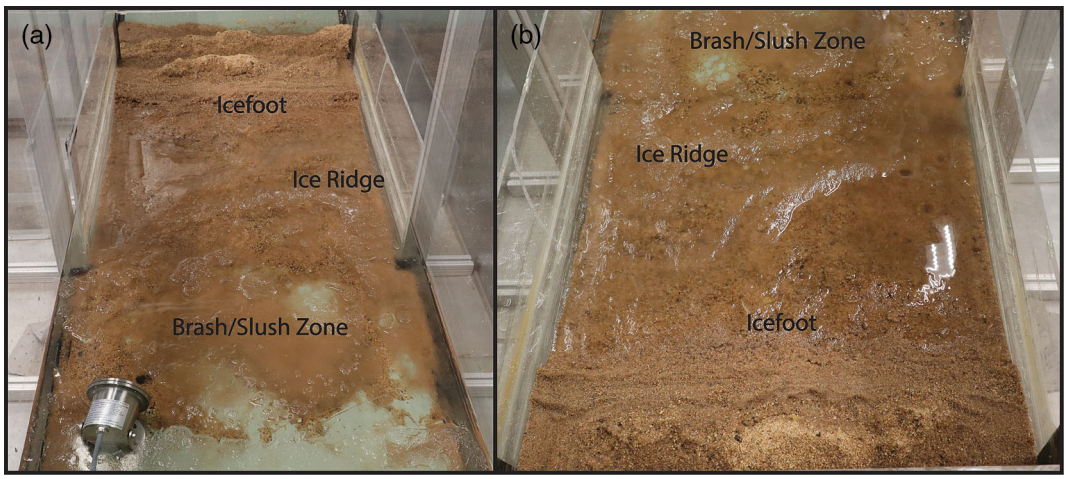

FIGURE 10 NIC breakup during the wave tank experiment with both thermal and mechanical processes. Both panels are from the same experiment (Experiment 2) but from different vantage points. Panel A is looking landward while Panel B is looking basinward. The width of the wave tank in each image is 0.6 m.

ice to be mostly deposited close to the ridge (Figure 7), rather than facilitating the formation of sediment-laden brash and slush that could be rafted offshore.

The ice lagoons initially degraded entirely from thermal processes, which is logical given the protection of the ice lagoon by the active ridges that were likely grounded to nearshore bars. The grounded ice of the passive ridges landward of the lagoon act as similar barriers. This creates isolated pooling of meltwater underneath the ice lagoon. The grounded ice on either side of the ice lagoon limits mixing with the colder open water and thus may locally warm. Thermal degradation is exacerbated because there is less sediment embedded in the lagoon ice than the ice ridge, and the ice is not frozen down to the lakebed (Bryan & Marcus, 1972). Furthermore, after there is an increased water content in the ice, its albedo will decrease leading to an increased melt rate and further weakening the ice. As the ice lagoon melts, a tabular, mud crack-like pattern emerges indicating weakening of the ice (Supplementary Figure S2). Once the outer ice ridge has been destroyed, this lagoon becomes active as it is exposed to the open lake. Mechanical forces become important in further deteriorating the ice lagoon as the ice ridge is no longer affording it protection. Wind and waves then work to efficiently destroy the ice lagoon. If offshore winds are present this ice and any entrained sediment are added to the brash ice floating offshore of the NIC (Supplementary Figures S2 and S3), potentially removing sediment from the nearshore.

The destruction of the inactive ice ridges, lagoons, and the icefoot processes are different because they are not exposed to as much mechanical forces as the active (outermost) ridge. This allows for thermal processes to melt much of the ice and results in some unique ice structures such as ice arches. By the time these ridges become 'active' and are exposed to mechanical forces and the open lake, they are likely no longer grounded, which would have provided some stability. Hinge cracks are common along the inactive ice ridge indicating weakening (Supplementary Figure S3). Since these ridges are weakened substantially by thermal processes, even a small wave event can efficiently destroy them. This was observed at the Chocolay site where the remaining inner ridges and grounded ice foot were destroyed quickly during a period of warming and a low magnitude (~2 m) onshore wave event, whereas previous events of such magnitude did not result in the NIC destruction. This has important implications for sediment transport as most of the sediment contained within the ice is deposited in place rather than being transported away from the breakup location.

The importance of thermal processes in facilitating ice breakup was confirmed with the wave tank experiments. NIC breakup was not possible in the wave tank with only wave action (i.e., mechanical forces) as was supported by $\Gamma \ll 1$. These waves only broke apart the ridges and lagoons when the temperature within the wave tank was increased and thermal degradation weakened the NIC. This produced a similar sequence of events as those observed in the field, where evidence for thermal weakening was initially observed and NIC breakup then proceeded primarily by mechanical processes. This also generated sediment transport behaviour in the wave tank that mirrored qualitative observations of sediment transport in the panoramic imagery. Apparent sediment deposition was documented in the Chocolay site panoramic images immediately basinward of the shoreline, which is likely primarily the result of thermal breakup (Figure 8). There also does appear to be pockets of sediment offshore of this primary depositional zone, which could be the result of coupled thermal and mechanical processes associated with NIC breakup.

Together these findings indicate that $h\sigma_y$ in Equation (2) should have an energy balance dependency ($h\sigma_y(E)$). That is when energy, E, inputted to the system (e.g., from turbulent and radiant surface fluxes and subsurface water temperatures) exceeds thermal cooling the excess energy will be used to melt the ice thereby thermally weaking it and reducing σ_y and h. In this manner waves that were not capable of breaking apart the NIC when $h\sigma_y$ was elevated now have sufficient force to break the NIC apart, effectively driving Γ towards unity by reducing F_s. The value of Γ estimated for the field wave data shown in Figure 5 produce $\Gamma = 0.14$ for wave heights of 1.2 m. The Γ from the wave tank experiments are ~4× smaller than those from the field but still within an order of magnitude indicating that the wave tank experiment did a reasonable job approximating the force balance from the field. However, in both instances the forces from the waves were much too small to break apart the NIC without thermally weaking the ice via reduction in $h\sigma_y$. The successful destruction of the NIC in Experiment 2 provides insights into the role of mechanical vs thermal affects, whereby thermal affects reduced the $h\sigma_y$ product by approximately 30-fold (which is what would be required to drive Γ towards unity). In the field the effect would only require a 7-fold reduction in $h\sigma_y$ and with the maximum waves observed (Figure 5, 2.4 m) only requires a 4-fold reduction in $h\sigma_y$. The possibility for such large reductions in strength from thermal degradation as observed in the wave tank experiments indicates that although thermal weakening is not strictly required for breakup, it represents a much more energetically efficient path when compared with the alternative of requiring extremely large waves.

4.2 | Conceptual model of NIC breakup processes

The field and laboratory observations in this study revealed that a combination of thermal and mechanical processes drive NIC breakup. This combination of processes is similar to those that were observed through field and remote sensing measurements of landfast ice decay in the Alaskan Arctic by Petrich et al. (2012). Thermal degradation is generally 2-fold, generating melt from both the ambient air as well as from the open surface water adjacent to the ice. One of the reasons that ice ridges form and can rise above the water surface is because they are in direct contact with the bed (Bryan & Marcus, 1972, Seibel et al., 1976). The water at depth in Lake Superior, similar to other cold-climate regions, is rarely below the freezing point; thus, the ice at the base of the ridge that is in contact with the lake water is temperate and as the lake begins to warm the excess heat melts the ridge from the basinward edge (Figure 11). This process begins to undercut the ice ridge, similar to cliff erosion processes, and can in some instances trigger collapse of the overhanging ridge. Previous studies have asserted that these ice-ridges form and breakup entirely due to mechanical processes such as wave action; however, in both our field observations and the wave tank experiments in this study, simply increasing the wave action without first thermally weakening the ice did not induce NIC breakup. No portion of the NIC was broken up in the wave tank experiment when only mechanical forces were exerted, an observation that supports the field findings. In the experiment where thermal

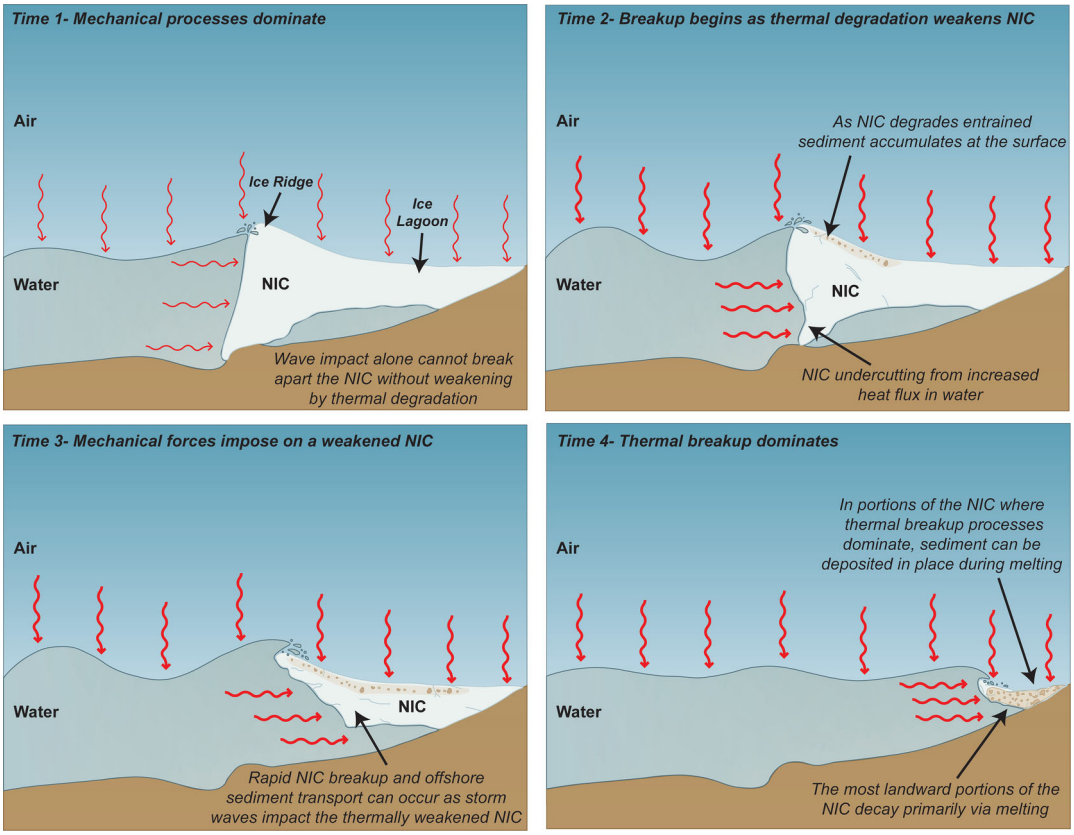

FIGURE 11 Conceptual model of NIC breakup. Heat energy leads to progressive weakening of the NIC, making it more susceptible to mechanical destruction via wave attack. The timing of these processes has important implications for where erosion occurs across the shoreface and whether sand is transported offshore or deposited in place when ice melts.

weakening was combined with the very same wave energy used to construct the NIC, widespread and relatively rapid destruction of the NIC occurred. This behaviour mimics the observations from the field at both locations and underscores the importance of thermal weakening in facilitating NIC breakup and associated sediment transport.

NIC breakup generally progresses from the open water towards the shoreline, although this does not proceed as uniformly as NIC buildup (Figure 11). This is due to thermal degradation from the water and ambient air acting over the entire NIC at the same time. The rate of breakup increases after the basal ice of the active ridge is no longer in contact with the bed. The active ice ridge is quickly consumed by the mechanical forces of the open water followed by the active ice lagoon and any other landward ice features. Once the icefoot is exposed to the open water, thermal degradation has weakened most of the ice within it. Over this breakup period, there was an increasing ratio of thermal to mechanical deterioration when moving landward in the NIC because components near the beach have had more time for thermal processes to weaken them by reducing $h\sigma_y$. Whether the ice is ultimately destroyed primarily by thermal or mechanical forces has important implications for the transport potential of the sediment embedded within the ice and whether it remains nearshore or is transported offshore.

The balance demonstrated in this study between thermal and mechanical processes for facilitating NIC breakup indicates that any future change in these conditions could have important implications for associated sediment transport and geomorphic changes along cold-climate coasts globally. A general decline in the prevalence of winter ice cover has been observed over the past century in cold-climate regions such as the Arctic and the Great Lakes of North America (Kumar et al., 2020; Wang et al., 2012). In particular, the length of the ice season is decreasing and the spatial extent of ice during the season is declining. For example, in the Great Lakes region since the 1970s, all the Great Lakes have documented both reductions in winter ice cover and increased variability in the timing of ice onset and breakup. As climate change continues to enhance warming throughout the region, the magnitude of ice impacts and associated coastal changes should increase, with the southern portion of the region likely experiencing these impacts first. This relationship can also be expected in the Arctic, with the southern Arctic being impacted first by enhanced ice variability. In Arctic marine environments, the presence of salt water could further amplify thermal degradation of the NIC by allowing salt rich brines to be emplaced atop the ice, thereby lowering the melting point, and causing surface melt to initiate at temperatures below those on the Great Lakes. Shore ice is clearly an important factor to consider when forecasting future changes along any cold coast due to ice's susceptibility to other climatic changes, such as increasing atmospheric and water temperatures and an increase in storminess (e.g., Nielsen et al., 2022). As shown in this study, the process of NIC breakup and the associated potential for nearshore sediment transport and morphology change is controlled by the ratio between thermal and mechanical processes. In a future climate scenario with enhanced meteorological extremes, it is conceivable that rapidly rising air and water temperatures at the end of a winter season may lead to rapid in-place deterioration of the NIC and local sediment deposition. In contrast, if enhanced storminess is observed during the late winter and spring storm season, it is possible that ice and associated sediment could be transported offshore,

potentially beyond the depth of closure. Given the role of thermal weakening for NIC breakup processes and the general trend of rising temperatures in cold-climate regions, shore ice breakup should be considered as an integral component of the overall morphodynamics of coasts in cold regions and one whose role is likely to be altered with climate change.

5 | CONCLUSIONS

Shore ice is a common feature during the winter along cold-climate coasts but the processes that govern its formation, breakup and associated sediment transport and geomorphic impact are poorly understood. This study combined field and laboratory methods to evaluate the relative importance of thermal and mechanical processes in facilitating NIC breakup. Field observations using UAS and panoramic ground imagery revealed that ice began to deteriorate only when atmospheric and lake water temperature rose above freezing. Wave events documented during the study period only facilitated NIC breakup when combined with an increase in thermal degradation. Wave tank experiments supported these observations as the NIC generated in the wave tank could not be broken apart purely by mechanical (i.e., wave) processes. Once the air and water temperatures were increased in the wave tank, the mechanical processes were able to erode the NIC. The ratio of thermal to mechanical processes at a given site have important implications for potential sediment transport pathways in response to NIC breakup. Purely thermal processes could result in sediment deposition in situ as the ice melts in place. A combination of thermal and mechanical processes efficiently destroys the NIC and could allow for sediment to be easily transported throughout the nearshore. If the right conditions occur during ice breakup, sediment may be transported offshore beyond the depth of closure. With future projections of increased atmospheric warming, it is probable that NIC breakup processes will play an increasingly important role in the dynamics of sediment transport and geomorphic change along cold coasts and should be considered in coastal evolution models and management planning.

AUTHOR CONTRIBUTIONS

Ethan J. Theuerkauf and Lucas K. Zoet were responsible for conceptualization, funding acquisition, methodology, investigation, resources, software, supervision and writing and editing the manuscript. Stefanie E. Dodge was responsible for methodology, investigation and writing and editing the manuscript. William Tuttle was responsible for investigation and editing the manuscript. J. Elmo Rawling III was responsible for conceptualization, funding acquisition and editing the manuscript.

ACKNOWLEDGEMENTS

The authors would like to thank Mary Debona for collecting the panoramic imagery at the Chocolay site and for drafting the conceptual model figure and Peter Sobol for assistance with the wave tank construction. Funding for this work was provided by the National Science Foundation [Award Numbers 1950101 (Theuerkauf) and 1916179 (Zoet and Rawling)—Collaborative Research: Sediment Transport Mechanisms and Geomorphic Processes Associated with Shore Ice along Cold Climate Coastlines].

DATA AVAILABILITY STATEMENT

Some of the data for this study are made available as supplementary online information including photographs and videos from the study. Other data from the wave tank experiments, drone data flights and panoramic image sets are maintained on MSU and University of Wisconsin-Madison servers and can be supplied to interested individuals by written request to the corresponding author.

ORCID

Ethan J. Theuerkauf https://orcid.org/0000-0002-9035-7454
Lucas K. Zoet https://orcid.org/0000-0002-9635-4051

REFERENCES

Bajorunas, L. & Duane, D.B. (1967) Shifting offshore bars and harbor shoaling. *Journal of Geophysical Research*, 72(24), 6195–6205. Available from: https://doi.org/10.1029/JZ072i024p06195

BaMasoud, A. & Byrne, M.-L. (2012) The impact of low ice cover on shoreline recession: a case study from Western Point Pelee, Canada. *Geomorphology*, 173–174, 141–148. Available from: https://doi.org/10.1016/j.geomorph.2012.06.004

Barnes, P.W., Kempema, E.W., Reimnitz, E. & McCormick, M. (1994) The influence of ice on southern Lake Michigan coastal erosion. *Journal of Great Lakes Research*, 20(1), 179–195. Available from: https://doi.org/10.1016/S0380-1330(94)71139-4

Barnes, P.W., Kempema, E.W., Reimnitz, E., McCormick, M., Weber, W.S. & Hayden, E.C. (1993) Beach profile modification and sediment transport by ice: an overlooked process on Lake Michigan. *Journal of Coastal Research*, 9(1), 65–86.

Bryan, M.L. & Marcus, M.G. (1972) Physical characteristics of near-shore ice ridges. *Arctic*, 25(3), 182–192. Available from: https://doi.org/10.14430/arctic2960

Dodge, S.E., Zoet, L.K., Rawling, J.E. III, Theuerkauf, E.J. & Hansen, D.D. (2022) Transport properties of fast ice within the nearshore. *Coastal Engineering*, 177. Available from: https://doi.org/10.1016/j.coastaleng.2022.104176

Evenson, E.B. & Cohn, B.P. (1979) The ice-foot complex; its morphology, formation and role in sediment transport and shoreline protection. *Zeitschrijt Fur Geomorphologie*, 23, 58–75.

Farquharson, L.M., Mann, D.H., Swanson, D.K., Jones, B.M., Buzard, R.M. & Jordan, J.W. (2018) Temporal and spatial variability in coastline response to declining sea-ice in northwest Alaska. *Marine Geology*, 404, 71–83. Available from: https://doi.org/10.1016/j.margeo.2018.07.007

Forbes, D.L. & Taylor, R.B. (1994) Ice in the shore zone and the geomorphology of cold coasts. *Progress in Physical Geography: Earth and Environment*, 18(1), 59–89. Available from: https://doi.org/10.1177/030913339401800104

Hubertz, J.M. (1992) *User's guide to the wave information studies (WIS) wave mode, version 2.0*. Vicksburg, MS, USA: Coastal Engineering Research Center United States Army Corps of Engineers. Available from: https://apps.dtic.mil/sti/citations/ADA254313

Irrgang, A.M., Bendixen, M., Farquharson, L.M., Baranskaya, A.V., Erikson, L.H., Gibbs, A.E. et al. (2022) Drivers, dynamics and impacts of changing Arctic coasts. *Nature Reviews Earth & Environment*, 3(1), 39–54. Available from: https://doi.org/10.1038/s43017-021-00232-1

Kelsch, M. & Goldstein, L. (2010) *River ice processes—short version: ice cover breakup: mechanical. Understanding the hydrologic cycle.* Available from: http://ftp.comet.ucar.edu/memorystick/hydro/basic_int/river_ice/navmenu.php_tab_1_page_23.0.0.htm

Kumar, A., Yadav, J. & Mohan, R. (2020) Global warming leading to alarming recession of the Arctic sea-ice cover: insights from remote sensing observations and model reanalysis. *Heliyon*, 6(7), E04355. Available from: https://doi.org/10.1016/j.heliyon.2020.e04355

Lantuit, H., Atkinson, D., Paul Overduin, P., Grigoriev, M., Rachold, V., Grosse, G. et al. (2011) Coastal erosion dynamics on the permafrost-

dominated Bykovsky Peninsula, north Siberia, 1951–2006. *Polar Research*, 30(1), 7341. Available from: https://doi.org/10.3402/polar.v30i0.7341

Manson, G.K., Davidson-Arnott, R.G.D. & Ollerhead, J. (2016) Attenuation of wave energy by nearshore sea ice: Prince Edward Island, Canada. *Journal of Coastal Research*, 32(2), 253. Available from: https://doi.org/10.2112/JCOASTRES-D-14-00207.1

Marsh, W.M., Marsh, B.D. & Dozier, J. (1973) Formation, structure, and geomorphic influence of Lake Superior icefoots. *American Journal of Science*, 273(1), 48–64. Available from: https://doi.org/10.2475/ajs.273.1.48

Mattheus, C.R., Diggins, T.P., Boyce, C., Cockrell, J., Kruske, M. & VanWinkle, M. (2019) Geomorphology of a harbor-breakwater beach along a high sand-supply, wave-dominated Great Lakes littoral cell. *Journal of Coastal Research*, 35(1), 41–55. Available from: https://doi.org/10.2112/JCOASTRES-D-17-00209.1

Miner, J.J. & Powell, R.D. (1991) An evaluation of ice-rafted erosion caused by an icefoot complex, southwestern Lake Michigan, U.S.A. *Arctic and Alpine Research*, 23(3), 320–327. Available from: https://doi.org/10.1080/00040851.1991.12002851

Mitsuyasu, H. (1962) Experimental study on wave force against a wall. *Coastal Engineering. Japan*, 5(1), 23–47. Available from: https://doi.org/10.1080/05785634.1962.11924617

Nielsen, D.M., Pieper, P., Barkhordarian, A., Overduin, P., Ilyina, T., Brovkin, V. et al. (2022) Increase in Arctic coastal erosion and its sensitivity to warming in the twenty-first century. *Nature Climate Change*, 12(3), 263–270. Available from: https://doi.org/10.1038/s41558-022-01281-0

O'Hara, N.W. & Ayers, J.C. (1972) Stages of shore ice development. In: *Proceedings 15th conference on Great Lakes research*. Ann Arbor, MI: International Association of Great Lakes Research, pp. 521–535.

Petrich, C., Eicken, H., Zhang, J., Krieger, J., Fukamachi, Y. & Ohshima, K.I. (2012) Coastal landfast sea ice decay and breakup in northern Alaska: key processes and seasonal prediction. *Journal of Geophysical Research, Oceans*, 117, C02003. Available from: https://doi.org/10.1029/2011jc007339

Seibel, E., Carlson, C.T. & Maresca, J.W. (1976) Ice ridge formation: probable control by nearshore bars. *Journal of Great Lakes Research*, 2(2), 384–392. Available from: https://doi.org/10.1016/S0380-1330(76)72301-3

Theuerkauf, E., Mattheus, C.R., Braun, K. & Bueno, J. (2021) Patterns and processes of beach and foredune geomorphic change along a Great Lakes shoreline: insights from a year-long drone mapping study along Lake Michigan. *Shore & Beach*, 89(2), 46–55. Available from: https://doi.org/10.34237/1008926

Wang, J., Bai, X., Hu, H., Clites, A., Colton, M. & Lofgren B. (2012) Temporal and spatial variability of Great Lakes ice cover, 1973-2010. *Journal of Climate*, 25(4). Available from: https://doi.org/10.1175/2011JCLI4066.1

Wang, J., Kessler, J., Bai, X., Clites, A., Lofgren, B., Assuncao, A. et al. (2018) Decadal variability of Great Lakes ice cover in response to AMO and PDO, 1963–2017. *Journal of Climate*, 31(18), 7249–7268. Available from: https://doi.org/10.1175/JCLI-D-17-0283.1

Westoby, M.J., Brasington, J., Glasser, N.F., Hambrey, M.J. & Reynolds, J.M. (2012) 'Structure-from-Motion' photogrammetry: a low-cost, effective tool for geoscience applications. *Geomorphology*, 179, 300–314. Available from: https://doi.org/10.1016/j.geomorph.2012.08.021

SUPPORTING INFORMATION

Additional supporting information can be found online in the Supporting Information section at the end of this article.

How to cite this article: Theuerkauf, E.J., Zoet, L.K., Dodge, S.E., Tuttle, W. & Rawling, J.E. III (2023) Nearshore ice complex breakup is controlled by a balance between thermal and mechanical processes. *Earth Surface Processes and Landforms*, 1–15. Available from: https://doi.org/10.1002/esp.5698